Ribosome assembly factor PNO1 is associated with progression and promotes tumorigenesis in triple-negative breast cancer

JIE LI[1-3*], LIYA LIU[1,2*], YOUQIN CHEN[4*], MEIZHU WU[1,2], XIAOYING LIN[1,2], ZHIQING SHEN[1,2], YING CHENG[1,2], XIAOPING CHEN[1,2], NATHANIEL WEYGANT[1,2], XIANGYAN WU[1,2], LIHUI WEI[1,2], THOMAS J. SFERRA[4], YUYING HAN[1,2], XI CHEN[3], ALING SHEN[1,2] and JUN PENG[1,2]

[1]Academy of Integrative Medicine and [2]Fujian Key Laboratory of Integrative Medicine on Geriatrics, Fujian University of Traditional Chinese Medicine, Fuzhou, Fujian 350122; [3]Department of Oncology, No. 900 Hospital of The Joint Logistic Support Force, Fuzhou, Fujian 350025, P.R. China; [4]Department of Pediatrics, Case Western Reserve University School of Medicine, Rainbow Babies and Children's Hospital, Cleveland, OH 44106, USA

Received October 4, 2021; Accepted January 14, 2022

DOI: 10.3892/or.2022.8319

Abstract. The aim of the present study was to investigate the expression of ribosome assembly factor partner of NOB1 homolog (PNO1) and its association with the progression of breast cancer (BC) in patients, as well as its biological function and underlying mechanism of action in BC cells. Bioinformatics and immunohistochemical analyses revealed that PNO1 expression was significantly increased in BC tissues and its high mRNA expression was associated with shorter overall survival (OS) and relapse-free survival (RFS) of patients with BC, as well as multiple clinical characteristics (including advanced stage of NPI and SBR, etc.) of patients with BC. Biological functional studies revealed that transduction of lentivirus encoding sh-PNO1 significantly downregulated PNO1 expression, reduced cell confluency and the number of BC cells *in vitro* and inhibited tumor growth *in vivo*. Moreover, PNO1 knockdown decreased the cell viability and arrested cell cycle progression at the G2/M phase, as well as down-regulated cyclin B1 (CCNB1) and cyclin-dependent kinase 1 (CDK1) protein expression in BC cells. Correlation analysis demonstrated that PNO1 expression was positively correlated with both CDK1 and CCNB1 expression in BC samples. Collectively, PNO1 was upregulated in BC and associated with BC patient survival, and PNO1 knockdown suppressed tumor growth *in vitro* and *in vivo*. In addition, positive regulation of CCNB1 and CDK1 may be one of the underlying mechanisms.

Correspondence to: Dr Aling Shen or Professor Jun Peng, Academy of Integrative Medicine, Fujian University of Traditional Chinese Medicine, 1 Qiuyang, Minhou, Shangjie, Fuzhou, Fujian 350122, P.R. China
E-mail: saling86@hotmail.com
E-mail: pjunlab@hotmail.com

*Contributed equally

Abbreviations: BC, breast cancer; RFS, relapse-free survival; OS, overall survival; IHC, immunohistochemistry; TCGA, The Cancer Genome Atlas; TMA, tissue microarray; PCR, polymerase chain reaction; STR, short tandem repeat; NPI, Nottingham prognostic index; SBR, Scarff-Bloom-Richardson; HER2, human epidermal growth factor receptor 2; PR, progesterone receptor; ER, estrogen receptor; CRC, colorectal cancer; DMEM, Dulbecco's modified Eagle's medium; TNBC, triple-negative breast cancer; GAPDH, glyceraldehyde 3-phosphate dehydrogenase; CDK1, cyclin-dependent kinase 1; PBS, phosphate-buffered saline

Key words: partner of NOB1 homolog, breast cancer, survival, tumor growth, cell cycle

Introduction

The incidence and mortality of breast cancer (BC) are rapidly increasing worldwide (1-3). Among females, breast cancer is the most commonly diagnosed cancer (24.2% of total cancer cases) and the leading cause of cancer mortality (15.0% of total cancer deaths) (4). Although surgical resection combined with chemotherapy and radiotherapy has been widely applied in patients with BC, therapeutic outcomes remain unsatisfactory (5). Despite the fact that it has been proven that BC development and/or progression is closely associated with a number of genetic alterations, the molecular pathogenesis has not been fully elucidated. Therefore, understanding the molecular profiles of BC as well as elucidating the role of genetic changes involved in BC may lead to novel therapeutic strategies for individual patients with BC (6,7).

Ribosome biogenesis is a complex process involving the synthesis and processing of pre-ribosomal RNAs, coordinated ribosome protein synthesis, and ribosome subunit assembly and transport. Moreover, ribosome assembly is highly dynamic and tightly linked to cell growth and proliferation (8-10). Mounting evidence reveals that both upregulation of ribosome biogenesis and intrinsic dysfunctions in ribosomes support increased cancer risk (11). In addition, a series of epidemiologic

observations and population-based studies has highlighted the importance of the association between ribosome biogenesis and cancer, including BC (12,13). In eukaryotes, the assembly of the ribosomal subunits is facilitated by more than 200 assembly factors including helicases, ATPases, GTPases, and kinases (14-17). In the absence of just one of these proteins, ribosome biogenesis is stalled, and cell growth is terminated even under optimal growth conditions (18-20). Defects in ribosome assembly and its regulation underlie many human diseases, including cancer (21,22). Previous observations have revealed that the upregulation of the ribosome assembly pathway is a hallmark of human cancers (23).

Ribosome assembly factor partner of NOB1 homolog (PNO1; Gene ID: 56902) has been revealed to be overexpressed in colorectal cancer (CRC) cells and associated with poor overall survival (OS) (24). Knockdown of PNO1 suppressed CRC growth *in vitro* and *in vivo* by inhibition of ribosome biogenesis and activation of the p53/p21 signaling pathway (24). However, the role of PNO1 in BC remains largely unknown. To explore the role of PNO1 in BC, bioinformatics and immunohistochemistry-based tissue microarray analyses were used to demonstrate that both the mRNA and protein levels of PNO1 were increased in BC compared to normal breast tissue. Moreover, the anti-tumorigenic effects of PNO1 knockdown *in vitro* and *in vivo* were demonstrated by determining the cell viability, cell cycle progression, as well as the expression of relative proteins. The present study provided further insight into the role of PNO1 in BC and suggest its potential use as a prognostic/diagnostic marker for BC.

Materials and methods

Bioinformatics analyses. Oncomine, an online cancer microarray database collecting gene expression array datasets, was queried to assess PNO1 mRNA expression in BC and noncancerous breast tissues. The expression of PNO1 in 3 different datasets (25,26) including the Curtis *et al* breast cancer dataset, the Zhao *et al* breast cancer dataset and The Cancer Genome Atlas (TCGA), were analyzed and presented using scatter plots in the present study. Data analysis was performed according to standardized normalization techniques and statistical calculations provided by the Oncomine website. The Kaplan-Meier plotter (www.kmplot.com), containing gene expression data and survival information of patients with BC, was queried to analyze the association between PNO1 mRNA expression and survival of patients with BC, including OS and RFS. The expression of PNO1 among the samples was divided into high or low groups according to the median expression, and the association of PNO1 expression with the survival of patients with BC was analyzed using the log-rank test method.

The R2 application (http://r2.amc.nl) was used to explore the association between PNO1 expression and RFS of patients with BC (dataset: Tumor Breast (Relapse)-Smid-210-MAS5.0-u133p2; GEO ID: GSE29271) using the log-rank method, and the correlation of PNO1 mRNA expression with CDK1 and CCNB1 was assessed using the Pearson correlation method.

To explore the potential prognostic impact of PNO1 in human BC, online analysis through bc-GenExMiner v4.0 (http://bcgenex.ico.unicancer.fr/BC-GEM/GEM-Accueil.php?js=1) was conducted to compare target gene expression according to clinical criteria (27,28). The association between PNO1 expression with clinicopathological parameters (including hormonal receptors, nodal status and other factors) were evaluated.

Reagent and antibodies. Fetal bovine serum (FBS), trypsin-EDTA (0.25%), Pierce™ BCA Protein Assay kit, FxCycle™ PI/RNase Staining Solution and Dulbecco's modified Eagle's medium (DMEM) were purchased from Thermo Fisher Scientific, Inc. L-15 medium containing 80 U/ml penicillin and 80 μg/ml streptomycin (Nanjing KeyGen Biotech Co., Ltd.) was used to culture MDA-MB-231 cells. Western and IP Lysis Buffer were acquired from Beyotime Institute of Biotechnology. CCK-8 and antibody for glyceraldehyde 3-phosphate dehydrogenase (GAPDH; polyclonal; cat. no. ABP57259) were obtained from Abbkine, Inc. Matrigel was purchased from BD Biosciences. Cyclin B1 polyclonal (product no. 4138S) antibody and β-actin monoclonal (product no. 4970S) antibody were purchased from Cell Signaling Technology, Inc. CDK1 monoclonal (product code ab18) antibody was purchased from Abcam. PNO1 antibodies were purchased from LSBio, Inc. (polyclonal; cat. no. LS-C179090) and Santa Cruz Biotechnology, Inc. (monoclonal; cat. no. sc-514727) respectively. Goat anti-rabbit IgG HRP-conjugated secondary antibody (cat. no. L3012) and goat anti-mouse HRP-conjugated IgG secondary antibody (cat. no. L3032) were purchased from Signalway Antibody LLC.

Immunohistochemistry (IHC)-based tissue microarray. TMA slides containing BC (cat. no. HBreD145Su01; n=145), or noncancerous adjacent breast tissues (cat. no. HBre-Duc090Sur-01; n=90) were purchased from Shanghai Outdo Biotech Company Co., Ltd. The specimens were obtained from Taizhou Hospital of Zhejiang Province (Zhejiang, China) from January 2001 to July 2013 (approval no. SHYJS-CP-1807007). IHC was performed to detect PNO1 (dilution 1:500; cat. no. LS-C179090; LSBio, Inc.) expression in clinical samples, followed by scoring using a grading system based on staining intensity as previously described (24,29). Staining intensity was assessed using a four-point scale (0, undetectable; 1, weak; 2, moderate; 3, strong), while the percentage of positively stained cells was expressed as one of four categories (0-25, 26-50, 51-75 and 76-100%). The final score was calculated as intensity score x percentage area score. The research was carried out according to the World Medical Association Declaration of Helsinki.

Cell culture and transduction. Human triple-negative breast cancer (TNBC) cell lines MDA-MB-231 (cat. no. TCHu227) and HS578T (cat. no. TCHu127) were purchased from the Cell Bank of the Chinese Academy of Sciences. MDA-MB-231 cells were maintained in L-15 medium supplemented with 10% FBS, and incubated at 37˚C in a humidified atmosphere containing 5% CO_2. HS578T cells were cultured in DMEM medium supplemented with 10% FBS and 100 U/ml penicillin, and 100 μg/ml streptomycin (Hyclone; Cytiva). The cells were verified using short tandem repeat (STR) genotyping and examined for *Mycoplasma* contamination using polymerase chain reaction (PCR) analysis according to the

manufacturer's instructions (MycoFree™ Mycoplasma detection kit; cat. no. GCMF82801QS; Shanghai GeneChem, Co., Ltd.). Briefly, the cells were collected and amplified by PCR, and then the sample was detected by agarose gel electrophoresis. The sequences of primers are listed in Table SI. The cell line was characterized by Genetic Testing Biotechnology Corporation using STR markers.

The generation system used was the 2nd and 293T cells were used as the interim cell line. To infect the plasmid, 293T cells were sub-cultured and seeded into 10-cm plates at a density of $5x10^6$ cells/15 ml. The medium was replaced with serum-free medium 2 h before transfection. The DNA solution including GV vector plasmid 20 μg, pHelper 1.0 carrier plasmid 15 μg, pHelper 2.0 vector plasmid 10 μg and corresponding volume of transfection reagent were evenly mixed. The total volume was adjusted to 1 ml and incubated at room temperature for 15 min. The medium was changed after 6 h of transduction and 10 ml PBS was added once. Subsequently, 20 ml fresh medium was added and the cells were incubated at 37˚C in a humidified atmosphere containing 5% CO_2 for an additional 48-72 h. For cell transduction, MDA-MB-231 and HS578T cells were sub-cultured and seeded into 12-well plates at a density of $0.4x10^5$ cells/well, and cultured overnight. Equivalent lentivirus coding short hairpin (sh)RNA targeting PNO1 (LV-PNO1-RNAi (14768): GIDL74453) or sh-Ctrl (CON053; hU6-MCS-CMV-EGFP: GCPL0169334; both from Shanghai GeneChem Co., Ltd.) was added at a multiplicity of infection (MOI) of 10. The double-stranded shRNAs for PNO1 are presented in Table SII. The medium was changed after 12 h of transduction and fresh medium was added. Cells were incubated at 37˚C in a humidified atmosphere containing 5% CO_2 for an additional 60 h before experiments were performed.

Cell confluence observation and cell number counting. The confluence of transduced cells was observed using light microscope (Leica Microsystems GmbH) and the representative images were obtained at a magnification of x200. The cells were then collected and the number of cells was calculated after staining with 0.4% Trypan blue for 3 min at room temperature using Countstar Automatic Cell Counting Apparatus (Shanghai ALIT Life Science).

Proliferation assay. At the end of the transduction, cells were reseeded in 96-well plates at a density of $0.2x10^4$ cells/well and cultured at 37˚C in a 5% CO_2 humidified incubator. Cell viability was examined at 24, 48, 72, 96 or 120 h using CCK-8 assay (Abbkine, Inc.). Briefly, 10 μl of CCK-8 was added to each well, and plates were incubated for an additional 2 h at 37˚C, followed by the measurement of the absorbance at 450 nm using an Infinite 200 Pro microplate reader (Tecan Group, Ltd.). The cell viability of both sh-Ctrl and sh-PNO1 on day 1 were set as 1 and the cell viability changes were present as the fold change relative to day 1.

Colony formation assay. The transduced cells were collected and reseeded in 12-well plates at a density of 500 cells/well. Cells were cultured for 12 days at 37˚C in a 5% CO_2 humidified incubator. Culture medium was changed every 3 days. Colonies were fixed using formaldehyde (4%) for 20 min at room temperature and stained using crystal violet (0.01%) for 20 min at room temperature. The number of colonies was counted manually and relative change in colony formation was determined.

Cell cycle analysis. Transduced MDA-MB-231 cells at a density of $1.0x10^5$ cells/well were fixed with 70% ethanol at 4˚C for 12-16 h. After washing with phosphate-buffered saline (PBS; Hyclone; Cytiva), cells were incubated with FxCycle PI/RNase Staining Solution for 30 min at room temperature, followed by analysis with FACSCaliber (BD Biosciences). The percentages of cells at different phases were analyzed using ModfitLT (version 3.0) (Verity Software House, Inc.).

In vivo xenograft assay. Male nude mice (4-6 weeks of age; 18-20 g) were purchased from Shanghai SLAC Laboratory Animal Co., Ltd. Transduced cells ($1x10^6$; sh-PNO1 or sh-Ctrl) in a total volume of 100 μl of PBS containing 50% Matrigel were injected subcutaneously into opposite flanks of individual mice (a total mice of n=6). The tumor volume was measured and recorded every 3 days from the 5th day after injection for a total of 43 days. The tumor volume was calculated with the following formula: $V=L \times W^2/2$. In order to observe whether the tumor affected the health status and weight of the mice, the behavior and health status of the mice were monitored every other day, and the mice were weighed every 3 days. The growth rate and volume of the tumor were observed, and whether the tumor was damaged and ulcerated was ascertained. The experiment would be terminated in advance when the tumor weight exceeded 10% of the body weight of the mouse, or the maximum diameter of the tumor of a 25-g mice exceeded 20 mm, or the animal was agitated or anxious, or the tumor was ulcerated or damaged. In our study, the experiment was terminated when the tumor volume reached 400-700 mm^3. At the end of the experiment, mice were anesthetized with an induction dose of 2% isoflurane and a maintenance dose of 1.5% isoflurane and tumor images were captured using an IVIS Spectrum live-animal imaging system (PerkinElmer, Inc.). After inhaling the induction and maintenance dose of 2% isoflurane into deep anesthesia, the mice (n=6) were then sacrificed by cervical dislocation. Confirmation of sacrifice was performed by verifying whether their heartbeat had stopped and their pupils were dilated, and then tumor tissues were collected and images were captured. All mice were housed in a pathogen-free environment with controlled temperature (22-26˚C), humidity (50-60%) and a 12-h light/dark cycle with *ad libitum* access to food and water. Animal care and experiments were performed in strict accordance with the 'Guide for the Care and Use of Laboratory Animals' of the National Research Council and the 'Principles for the Utilization and Care of Vertebrate Animals' of the National Institutes of Health and was approved (approval no. 2018-032) by the Animal Ethics Committee of Fujian University of Traditional Chinese Medicine (Fuzhou, China).

Western blot analysis. The transduced cells were collected and washed twice with PBS, and then lysed with 30-70 μl of lysis buffer supplemented with protease and phosphatase inhibitors. Protein concentration was determined by the BCA Protein assay. A total of 50 μg of protein was subjected to sodium dodecyl sulfate polyacrylamide gel electrophoresis (10%) and

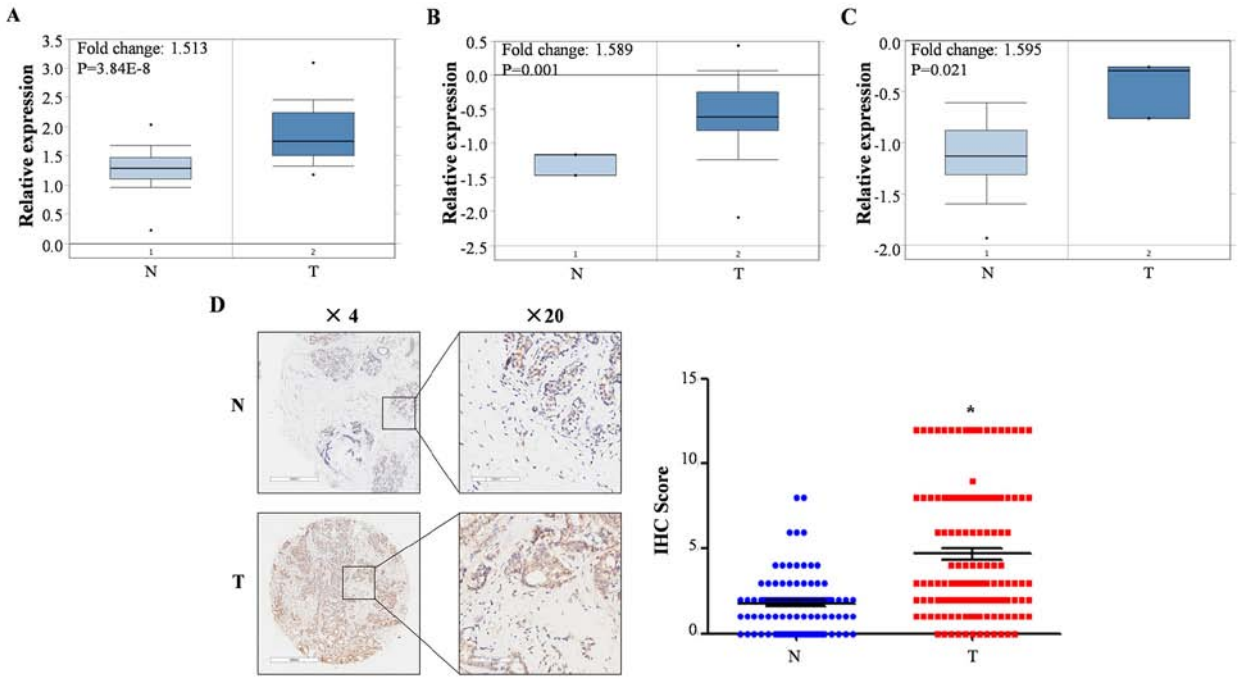

Figure 1. PNO1 is overexpressed in BC tissues. (A-C) PNO1 mRNA expression in BC tissues (T) and non-cancerous breast tissues (N) were analyzed in 3 different datasets using Oncomine and determined to be upregulated in BC (all P<0.05). (D) PNO1 protein expression was increased in BC tissues (T) compared to non-cancerous breast tissues (N) as determined by IHC using a tumor microarray. Representative images were obtained at magnifications of x4 or x20 (left panel); the composite score was calculated as the intensity score x the percentage area score (right panel). *P<0.05. PNO1, partner of NOB1 homolog; BC, breast cancer.

then transferred onto a polyvinylidene fluoride membrane (EMD Millipore). The resulting membrane was blocked using 5% milk in TBST buffer for 2 h at room temperature, and then incubated with primary antibodies PNO1, cyclin B1, CDK1, β-actin (all diluted 1:1,000), or GAPDH (dilution, 1:5,000) overnight at 4˚C, followed by incubation with secondary antibody (dilution, 1:5,000) for 2 h at room temperature. GAPDH or β-actin protein levels were used as a loading control. The protein bands were detected with a chemiluminescence kit (Abbkine, Inc.) using the Bio-Rad Chemi Doc XRS imaging system (Bio-Rad Laboratories, Inc.) and band intensities were quantified using ImageJ software (1.51j8; National Institutes of Health). The expression of GAPDH or β-actin was used as an internal control. The levels of the aforementioned proteins were calculated relative to the levels in sh-Ctrl cells, which was set as 1.00.

Statistics analysis. Experiments were performed at least in triplicate and data were presented as the mean ± standard deviation. Statistical analyses between groups were performed using the independent Student's t-test in SPSS 20.0 (IBM Corp.). P<0.05 (two sided) was considered to indicate a statistically significant difference.

Results

PNO1 is overexpressed at the mRNA and protein levels in BC. Analysis of PNO1 mRNA expression in breast cancer using Oncomine demonstrated that the mRNA expression of PNO1 in BC was significantly upregulated compared to non-cancerous adjacent breast tissues (Fig. 1A-C; P<0.05). IHC-based detection of PNO1 protein expression in BC (n=145) and non-cancerous breast tissues (n=90) demonstrated that the protein levels of PNO1 were significantly upregulated in BC (Fig. 1D; P<0.05). Clinicopathological characteristics of patients are summarized in Table SIII and revealed that no clinicopathological characteristics of the patients were significantly associated with PNO1 expression. These findings indicated that PNO1 was overexpressed at both the mRNA and protein levels of BC tissues.

High PNO1 expression predicts progression and shorter survival in patients with BC. Next, the association between mRNA expression of PNO1 and survival of patients with BC was investigated. High mRNA expression of PNO1 in BC tissues was significantly associated with reduced OS and RFS in patients with BC (Fig. 2A and B; P<0.05), which was consistent with the analyses of RFS using R2 application (Fig. 2C-E). Correlation analyses of PNO1 mRNA expression with various clinicopathological parameters were performed using bc-GenExMiner. As revealed in Fig. 3A, there were no obvious differences in PNO1 expression between patients >51 and ≤51 years old. In terms of nodal status in patients with BC, PNO1 expression was higher in those with positive nodal status compared to negative nodal status (Fig. 3B; P<0.05). Correlation between the progesterone receptor (PR) and estrogen receptor (ER) statuses of patients with BC revealed lower PNO1 expression in patients both with positive PR (Fig. 3C; P<0.05) and ER (Fig. 3D; P<0.05) status, while there was no significant difference between patients with human epidermal growth factor receptor 2 $(HER2)^-$ and $HER2^+$ BC (Fig. 3E; P>0.05). Moreover, the present study revealed that PNO1 expression was significantly increased in patients with TNBC (Fig. 3F; P<0.001). Analyses also found that PNO1

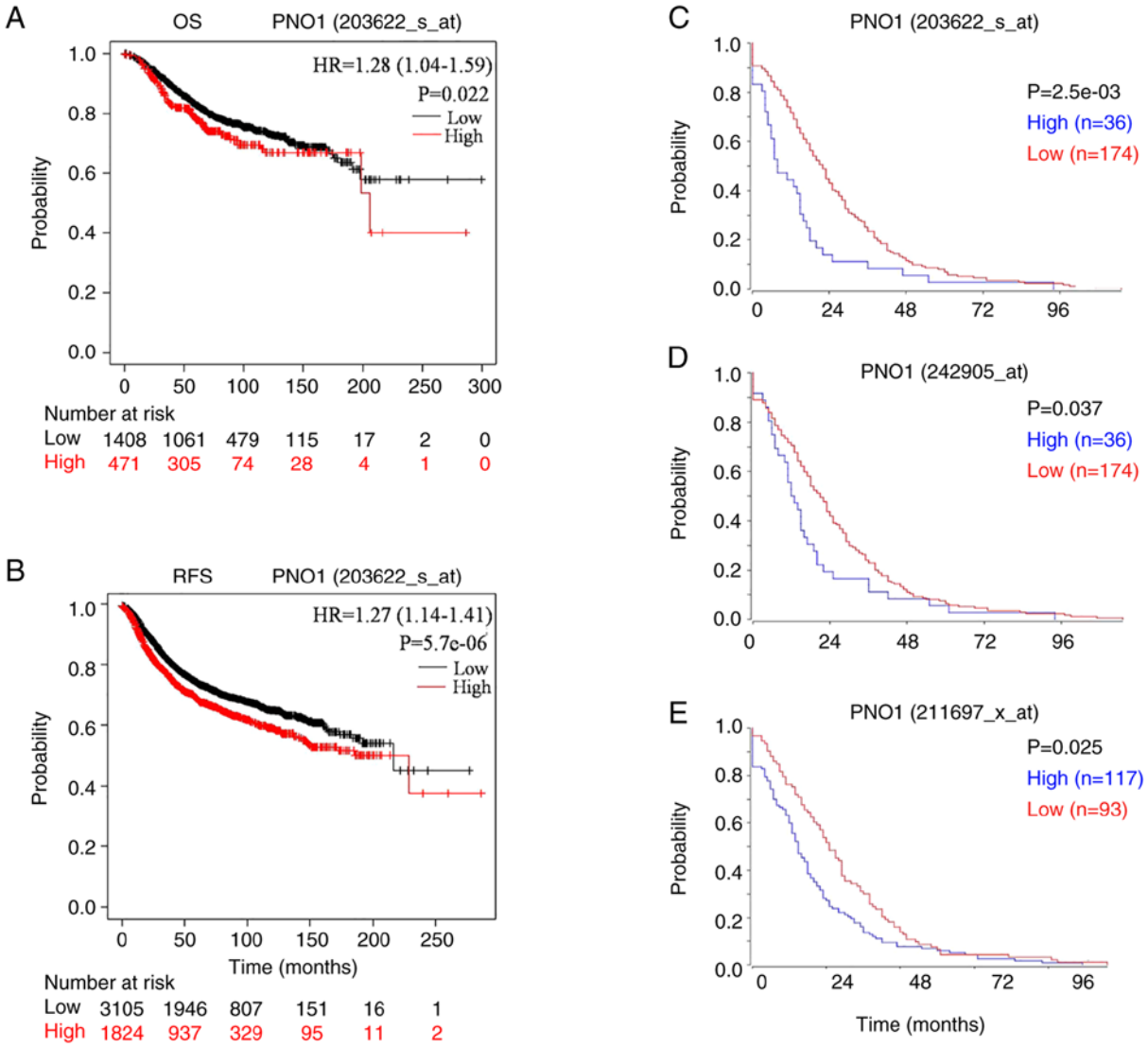

Figure 2. PNO1 expression is associated with the survival of patients with BC. The Kaplan-Meier plotter database was used to analyze the association between PNO1 mRNA expression and (A) OS and (B) RFS in patients with BC (both P<0.05). (C-E) A public clinical microarray dataset from the R2 bioinformatic platform was used to analyze the association between PNO1 mRNA expression and RFS of patients with BC (P<0.05). PNO1, partner of NOB1 homolog; BC, breast cancer; OS, overall survival; RFS, relapse-free survival.

expression was higher in patients with basal-like BC (Fig. 3G; P<0.05). With regard to Nottingham prognostic index (NPI) grade and Scarff-Bloom-Richardson (SBR) grading, it was determined that PNO1 expression was higher in advanced NPI grades (Fig. 3H; NPI2 and NPI3, both P<0.05, vs. NPI1) and SBR grades (Fig. 3I; SBR2 vs. SBR1, SBR3 vs. SBR1, SBR3 vs. SBR2, all comparisons P<0.05). These findings indicated that high PNO1 expression was correlated with progression of cancer in patients with BC.

PNO1 knockdown suppresses BC cell growth in vitro in vivo. The biological and functional role of PNO1 in BC through manipulation of gene expression, was next investigated. After knocking down PNO1 expression in human BC MDA-MB-231 and HS578T cells via shRNA-PNO1 lentivirus transduction (Fig. 4A; P<0.05), observation of cell growth by microscopy and cell number counting revealed that PNO1 knockdown significantly reduced cell confluence and the number of cells, in both MDA-MB-231 and HS578T cells (Fig. 4B; P<0.05). Further determination of cell viability by CCK-8 assay and cell survival by colony formation assay indicated that PNO1 knockdown significantly decreased cell viability (Fig. 4C; P<0.05) and the survival rate of BC cells (Fig. 4D; P<0.05).

The present study further assessed the biological function of PNO1 knockdown on tumor growth *in vivo*. During the experiment, no significant weight loss, tension, anxiety of mice or injury, or ulcer of tumor tissues was observed. Observation of tumors using an IVIS Spectrum whole live-animal imaging system, tumor volume measurements, endpoint determination of the tumor weight, and analysis of the intertumoral GFP fluorescence intensity of tumor tissues revealed that PNO1 knockdown in MDA-MB-231 cells attenuated tumor growth (Fig. 5A), significantly reduced the tumor volume (Fig. 5B), GFP fluorescence intensity (Fig. 5C and D), as well as tumor weight (Fig. 5E) in a xenograft nude mouse model (P<0.05 for all comparisons). Collectively, these findings demonstrated that PNO1 knockdown suppressed tumor growth of BC cells *in vivo*.

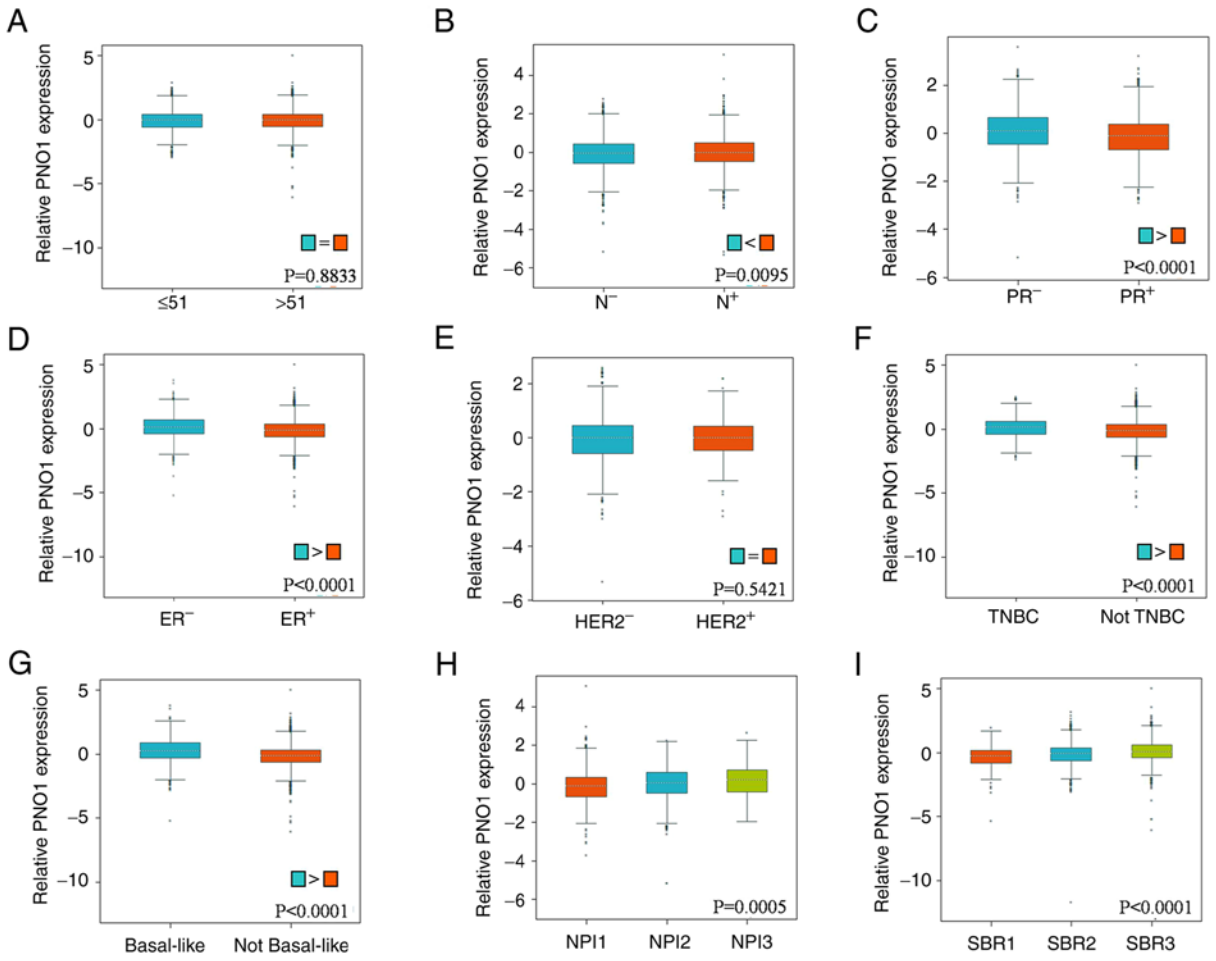

Figure 3. Correlation of PNO1 with clinicopathological parameters in BC patient tissues. Bc-GenExMiner was used to analyze the correlation of PNO1 with (A) age (P>0.05), (B) nodal status (P<0.05), (C) PR status (P<0.05), (D) ER status (P<0.05), (E) HER2 status (P>0.05), (F) TNBC status (P<0.05), (G) basal-like status (P<0.05), (H) NPI status (P<0.05 for NPI2 vs. NPI1 and NPI3 vs. NPI1) and (I) SBR (P<0.05 for SBR2 vs. SBR1, SBR3 vs. SBR1, and SBR3 vs. SBR2) based on PNO1 mRNA expression in BC tissues. PNO1, partner of NOB1 homolog; BC, breast cancer; PR, progesterone receptor; ER, estrogen receptor; HER2, human epidermal growth factor receptor 2; TNBC, triple-negative breast cancer; NPI, Nottingham prognostic index; SBR, Scarff-Bloom-Richardson.

PNO1 knockdown suppresses cell proliferation by downregulating cyclin B1 and CDK1. The effect of PNO1 on the BC cell cycle was investigated using PI staining followed by FACS analysis. As revealed in Fig. 6A, PNO1 knockdown significantly reduced the percentage of cells in both G0/G1 and S phases, while increasing the percentage of cells in the G2/M phase in MDA-MB-231 cells, suggesting that PNO1 knockdown arrests BC cell cycle progression at the G2/M phase. Further determination of the expression of G2/M-related proteins using western blot analysis indicated that PNO1 knockdown downregulated the expression of CDK1 and cyclin B1 (Fig. 6B; P<0.05). Correlation analysis of PNO1 indicated that its expression in BC was positively correlated with both CDK1 and CCNB1 at the mRNA level (Fig. 6C; P<0.05). These data indicated that the anti-proliferative effect of PNO1 knockdown was due to G2/M arrest via downregulation of CDK1 and cyclin B1 expression.

Discussion

The present study provided evidence for the essential role of PNO1 in BC. Database analysis and verification by IHC revealed that PNO1 expression was significantly increased in BC tissues at both the mRNA and protein levels when compared to non-cancerous breast tissues. Survival and clinicopathological analyses demonstrated that increased PNO1 was associated with shorter OS, RFS and multiple advanced clinical characteristics. Functional and mechanistic studies indicated that PNO1 knockdown suppressed BC cell growth *in vitro* and *in vivo* by inhibiting the proliferation of BC cells, which likely occurred via downregulation of CDK1 and cyclin B1 expression mediating G2/M-phase cell cycle arrest.

Recently, more than 200 ribosome assembly factors have been identified, some of which have been demonstrated to be hallmarks of cancers and play an essential role in uncontrolled proliferation of cancer cells, including NOB1 and RIO1 (30,31). Similar to these assembly factors, our previous data showed that PNO1 was critical for ribosome biogenesis in CRC cells (24), involved in tumor growth and progression of CRC by regulating the p53 signaling pathway. In the present study, focus was on verifying the clinical significance and function of PNO1 in BC. As expected, the expression of PNO1 was increased in BC tissues at both the mRNA and protein levels. Based on the expression of PNO1 in BC tissues, the correlation between its mRNA expression and clinical stage was analyzed. Unfortunately, significant differences between stages I-II and III-IV, were not obtained.

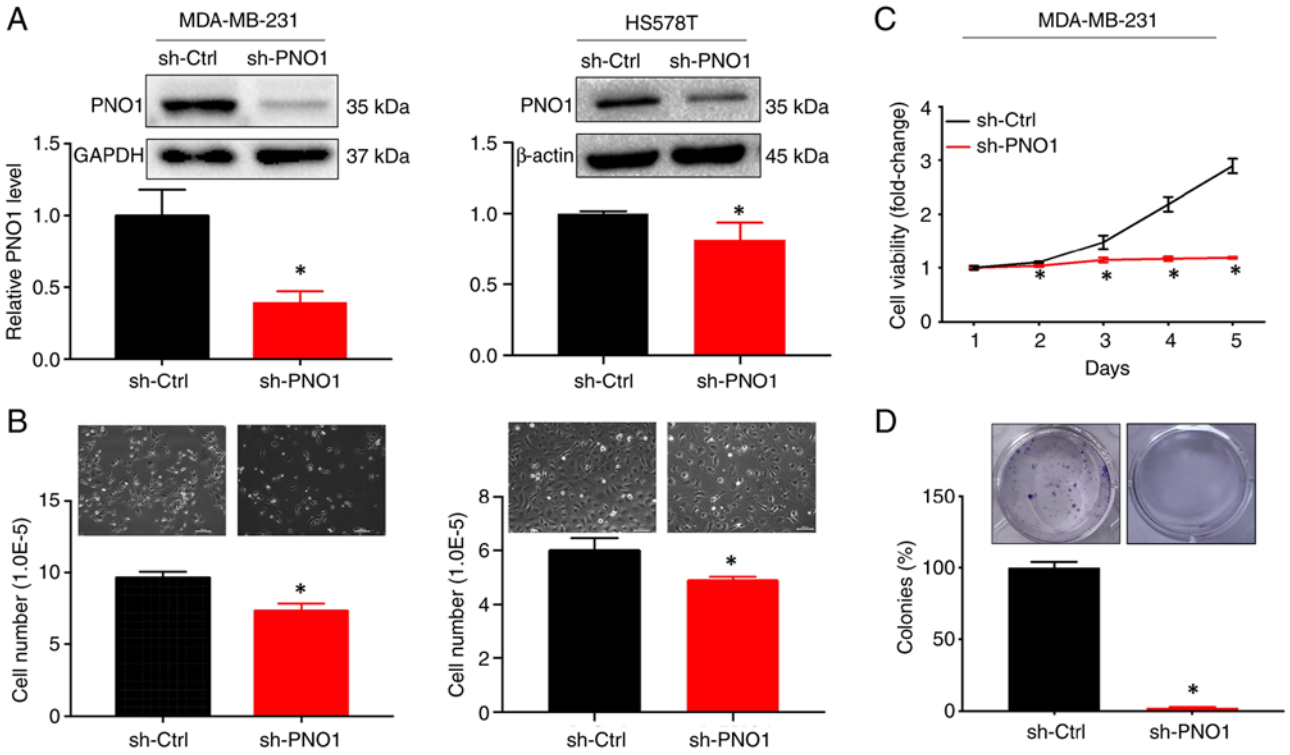

Figure 4. PNO1 knockdown suppresses BC cell growth *in vitro*. (A and B) MDA-MB-231 (left panel) or HS578T (right panel) cells were transduced with lentivirus encoding shRNA targeting PNO1. (A) Western blotting was performed to determine PNO1 protein expression. Bands were quantitated using ImageJ software, and normalized to GAPDH or β-actin. (B) Cell morphology was observed by microscopy at a magnification of x20 (upper panel), and the number of cells was counted using trypan blue exclusion (lower panel). (C) The cell viability of MDA-MB-231 cells was determined using the CCK-8 assay. Results were normalized to viability on day 1 and represented as the fold change. (D) Cell survival of MDA-MB-231 cells was assessed using a colony formation assay, and data were normalized to the survival of control cells. *P<0.05, vs. sh-Ctrl. PNO1, partner of NOB1 homolog; BC, breast cancer; CCK-8, Cell Counting Kit-8; sh-, short hairpin.

The expression of PNO1 in different types of BC tissues will be further addressed in our future study. Therefore, qPCR or western blot analyses will be further used to verify the expression of PNO1 in BC tissues after enough clinical samples from patients with BC are gathered.

Based on the high expression of PNO1 in BC tissues, the association between PNO1 expression and survival of patients with BC was further analyzed. The survival analysis demonstrated that increased PNO1 mRNA expression was significantly associated with shorter OS and RFS in patients with BC, which provided further evidence of the role of PNO1 in BC progression. However, an association between PNO1 protein expression and survival of patients with BC (data not shown) was not found, which may be due to limitations in the number of clinical samples. Furthermore, the correlation between PNO1 mRNA expression with various clinicopathological parameters was analyzed and it was determined that high PNO1 expression was correlated with lymph node metastasis, negative PR and ER, basal-like or TNBC status, and advanced SBR and NPI grades. The present study also analyzed the association between PNO1 protein expression and clinical characteristics of patients with BC based on its expression in BC tissues. Unfortunately, no significant association between PNO1 protein expression and all clinical characteristics was revealed, which may due to the limitations in the number of clinical samples. These findings provide further support for the oncogenic role of PNO1 and the possibility of using PNO1 as a biomarker for progression of BC.

Uncontrolled proliferation of cancer cells requires extensive protein synthesis and thus increased ribosome biogenesis (32). Therefore, the functional role of PNO1 in tumor growth was explored. Consistent with our previous study on CRC (18), PNO1 knockdown suppressed BC cell growth *in vitro* and *in vivo*. However, in a future study the suppressive effect of PNO1 knockdown on tumor growth *in vivo* will be verified using female nude mice, instead of male mice. Further determination of cell proliferation indicated that PNO1 knockdown attenuated cell viability and colony formation in BC cells. Our previous study found that PNO1 knockdown increased the percentage of CRC cells at G0/G1 phase (24). Unexpectedly, in the present study, PNO1 knockdown arrested BC cells in the G2/M phase, which may be due to variation in the status of cell cycle checkpoint regulators between cancer types or cell lines. In fact, the expression of G2/M-phase-related proteins was further detected and it was revealed that PNO1 knockdown downregulated CDK1 and cyclin B1 protein expression in BC cells. Moreover, PNO1 expression was positively correlated with both CDK1 and CCNB1 gene expression in patient tissue. Further studies should assess the underlying mechanisms involved in cell cycle differences between BC and CRC after PNO1 knockdown. Moreover, the role of PNO1 in different tumor types (BC and CRC, etc.) warrants further investigation. However, due to low expression of PNO1 in normal cells, the effect of PNO1 knockdown on cell proliferation was not detected. The effects of PNO1 knockdown and overexpression in normal cells will be verified in our future

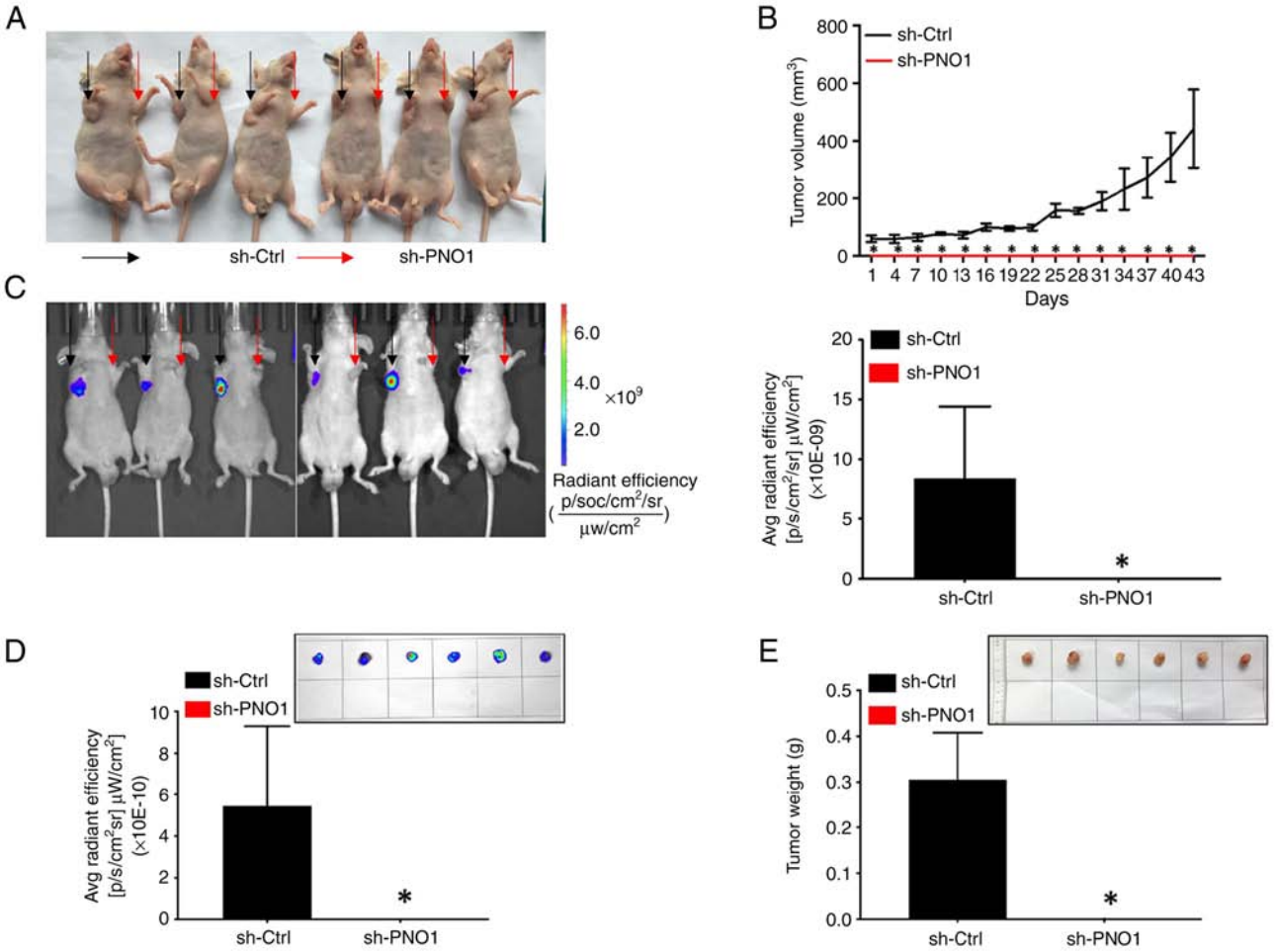

Figure 5. PNO1 knockdown suppresses BC tumor growth *in vivo*. A xenograft nude mouse model was used to assess the effect of PNO1 knockdown on tumor growth. Transduced MDA-MB-231 (sh-PNO1) cells were injected subcutaneously into opposite flanks of BALB/c mice. Images of tumors in opposite flanks of mice were obtained using (A) an electronic camera. (B) The average tumor volume was measured and recorded starting on the 5th day after injection. (C-D) IVIS Spectrum whole live-animal imaging system was used to obtain the image of tumor (left panel) and analyze the GFP intensity (right panel) (C) The representative images of fluorescence in tumors were observed by IVIS Spectrum whole live-animal imaging system (upper panel) and GFP intensity (lower panel) was analyzed (D). (E) Representative images of tumors (upper panel) were observed and the average tumor weight (lower panel) was assessed. *P<0.05, vs. sh-Ctrl. PNO1, partner of NOB1 homolog; BC, breast cancer; sh-, short hairpin.

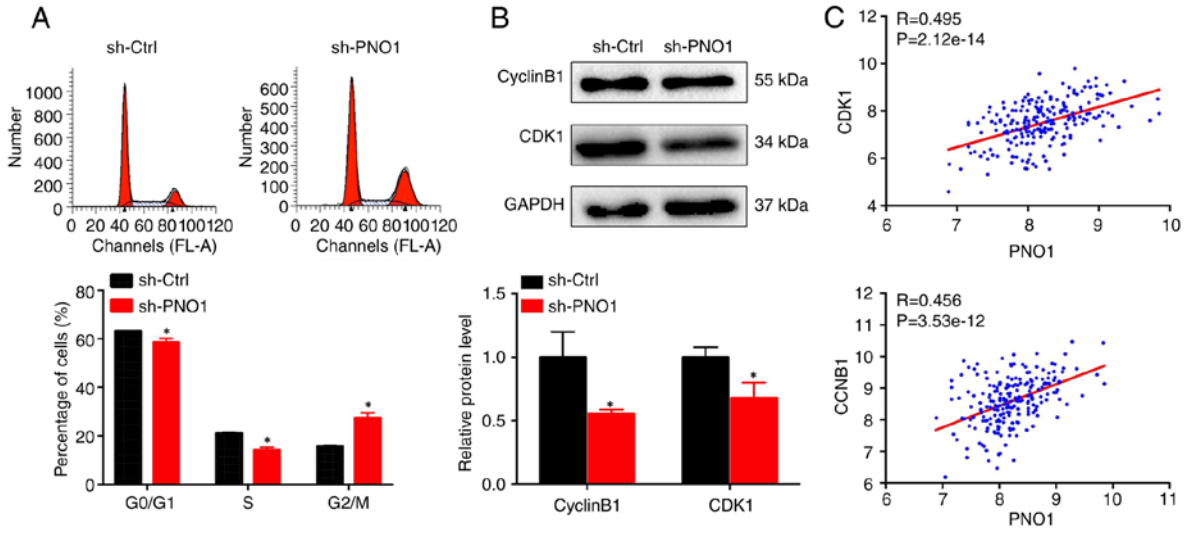

Figure 6. PNO1 knockdown arrests the BC cell cycle at the G2/M phase. (A) Cell cycle distribution of MDA-MB-231 cells after PNO1 knockdown was determined by flow cytometry (upper panel), and percentages of cells in G0/G1, S, or G2/M phases were determined (lower panel). (B) The protein expression of cyclin B1 and CDK1 in MDA-MB-231 cells after PNO1 knockdown was determined by western blot analysis. The integrated band density was determined using ImageJ, and GAPDH was used as the internal control. *P<0.05. (C) Correlation of PNO1 with CDK1 (left panel) and CCNB1 (right panel) were analyzed through the R2 website. PNO1, partner of NOB1 homolog; BC, breast cancer; CCNB1, cyclin B1; sh-, short hairpin.

study. Furthermore, the roles of PNO1 overexpression on cell proliferation *in vitro* and *in vivo* and PNO1 knockdown on cell apoptosis of BC cells, as well as its underlying mechanisms should be further addressed in a future study.

In summary, the present study revealed that PNO1 expression was overexpressed in BC tissues compared with noncancerous breast tissue, and high PNO1 expression was significantly associated with poor prognosis and progression of cancer in patients with BC. Our present study also demonstrated that PNO1 knockdown suppressed tumor growth *in vivo* and *in vitro* by inhibiting cell proliferation which was likely mediated by downregulation of CDK1 and cyclin B1 expression. The present study highlights the clinical significance and biological function of PNO1 in BC, suggesting that PNO1 may serve as a potential biomarker or therapeutic target for BC.

Acknowledgements

Not applicable.

Funding

This work was supported by the National Natural Science Foundation of China under grant nos. 81803882, 81673721 and 81703913, the International Cooperative Project of Fujian Department of Science and Technology under grant no. 2017I0007, the Natural Science Foundation of Fujian Province under grant no. 2017J01846, and the 100 Talents Program of Fujian Province (2018).

Availability of data and materials

The datasets used and/or analyzed during the current study are available from the corresponding author on reasonable request.

Authors' contributions

AS and JP conceived and designed the experiments, as well as confirm the authenticity of all the raw data. JL, YoC, LL, MW and NW conducted the bioinformatics analysis and immunohistochemistry-based tissue microarray analysis. JL, LL, YoC, XL and ZS conducted the cell culture, Cell Counting Kit-8 assay and colony formation assay. YoC, MW and YH conducted the cell cycle analysis. JL, XW, YiC, XiaC and XiC performed the animal experiments and analysis. YiC, XiaC and LW conducted the western blotting and the data analysis. MW and TJS conducted the statistical analysis and prepared the images of the figures. YoC, JL and AS wrote the manuscript. TJS, NW and JP revised the manuscript. All authors read and approved the manuscript and agree to be accountable for all aspects of the research in ensuring that the accuracy or integrity of any part of the work are appropriately investigated and resolved.

Ethics approval and consent to participate

The specimens were obtained from Taizhou Hospital of Zhejiang Province (Zhejiang, China) and approved by Ethics Committee of Shanghai Outdo Biotech Company (approval no. SHYJS-CP-1807007) with written informed consent from patients.

All animal maintenance and procedures were performed in strict accordance with the 'Guide for the Care and Use of Laboratory Animals' of the National Research Council and the 'Principles for the Utilization and Care of Vertebrate Animals' of the National Institutes of Health and approved by the Animal Ethics Committee of Fujian University of Traditional Chinese Medicine (Fuzhou, China) (approval no. 2018-032).

Patient consent for publication

Not applicable.

Competing interests

The authors declare that they have no competing interests.

References

1. Manthri RG, Jeepalem SM, Krishna Mohan VS, Bhargavi D, Hulikal N and Kalawat T: Metachronous second primary malignancies in known breast cancer patients on 18F-Fluoro-2-Deoxyglucose positron emission tomography-computerized tomography in a tertiary care center. Indian J Nucl Med 34: 284-289, 2019.
2. Hessami Arani S and Kerachian MA: Rising rates of colorectal cancer among younger Iranians: Is diet to blame? Curr Oncol 24: e131-e137, 2017.
3. Fahad Ullah M: Breast cancer: Current perspectives on the disease status. Adv Exp Med Biol 1152: 51-64, 2019.
4. Bray F, Ferlay J, Soerjomataram I, Siegel RL, Torre LA and Jemal A: Global cancer statistics 2018: GLOBOCAN estimates of incidence and mortality worldwide for 36 cancers in 185 countries. CA Cancer J Clin 68: 394-424, 2018.
5. Bernier J: Post-mastectomy radiotherapy after neodjuvant chemotherapy in breast cancer patients: A review. Crit Rev Oncol Hematol 93: 180-189, 2015.
6. Byler S, Goldgar S, Heerboth S, Leary M, Housman G, Moulton K and Sarkar S: Genetic and epigenetic aspects of breast cancer progression and therapy. Anticancer Res 34: 1071-1077, 2014.
7. Cobain EF, Milliron KJ and Merajver SD: Updates on breast cancer genetics: Clinical implications of detecting syndromes of inherited increased susceptibility to breast cancer. Semin Oncol 43: 528-535, 2016.
8. Boisvert FM, van Koningsbruggen S, Navascués J and Lamond AI: The multifunctional nucleolus. Nat Rev Mol Cell Biol 8: 574-585, 2007.
9. Brina D, Grosso S, Miluzio A and Biffo S: Translational control by 80S formation and 60S availability: The central role of eIF6, a rate limiting factor in cell cycle progression and tumorigenesis. Cell Cycle 10: 3441-3446, 2011.
10. Hang R, Liu C, Ahmad A, Zhang Y, Lu F and Cao X: Arabidopsis protein arginine methyltransferase 3 is required for ribosome biogenesis by affecting precursor ribosomal RNA processing. Proc Natl Acad Sci USA 111: 16190-16195, 2014.
11. Montanaro L, Trere D and Derenzini M: Changes in ribosome biogenesis may induce cancer by down-regulating the cell tumor suppressor potential. Biochim Biophys Acta 1825: 101-110, 2012.
12. Penzo M, Casoli L, Pollutri D, Sicuro L, Ceccarelli C, Santini D, Taffurelli M, Govoni M, Brina D, Trere D and Montanaro L: JHDM1B expression regulates ribosome biogenesis and cancer cell growth in a p53 dependent manner. Int J Cancer 136: E272-E281, 2015.
13. Catez F, Dalla Venezia N, Marcel V, Zorbas C, Lafontaine DLJ and Diaz JJ: Ribosome biogenesis: An emerging druggable pathway for cancer therapeutics. Biochem Pharmacol 159: 74-81, 2019.
14. Zemp I and Kutay U: Nuclear export and cytoplasmic maturation of ribosomal subunits. FEBS Lett 581: 2783-2793, 2007.
15. Strunk BS and Karbstein K: Powering through ribosome assembly. RNA 15: 2083-2104, 2009.
16. Kressler D, Hurt E and Bassler J: Driving ribosome assembly. Biochim Biophys Acta 1803: 673-283, 2010.

17. Rodriguez-Galan O, Garcia-Gomez JJ and de la Cruz J: Yeast and human RNA helicases involved in ribosome biogenesis: Current status and perspectives. Biochim Biophys Acta 1829: 775-790, 2013.
18. Iadevaia V, Liu R and Proud CG: mTORC1 signaling controls multiple steps in ribosome biogenesis. Semin Cell Dev Biol 36: 113-120, 2014.
19. Pelletier J, Thomas G and Volarevic S: Ribosome biogenesis in cancer: New players and therapeutic avenues. Nat Rev Cancer 18: 51-63, 2018.
20. Vizoso-Vazquez A, Barreiro-Alonso A, Gonzalez-Siso MI, Rodriguez-Belmonte E, Lamas-Maceiras M and Cerdan ME: HMGB proteins involved in TOR signaling as general regulators of cell growth by controlling ribosome biogenesis. Curr Genet 64: 1205-1213, 2018.
21. Freed EF, Bleichert F, Dutca LM and Baserga SJ: When ribosomes go bad: Diseases of ribosome biogenesis. Mol Biosyst 6: 481-493, 2010.
22. Armistead J and Triggs-Raine B: Diverse diseases from a ubiquitous process: The ribosomopathy paradox. FEBS Lett 588: 1491-1500, 2014.
23. Stumpf CR and Ruggero D: The cancerous translation apparatus. Curr Opin Genet Dev 21: 474-483, 2011.
24. Shen A, Chen Y, Liu L, Huang Y, Chen H, Qi F, Lin J, Shen Z, Wu X, Wu M, *et al*: EBF1-mediated upregulation of ribosome assembly factor PNO1 contributes to cancer progression by negatively regulating the p53 signaling pathway. Cancer Res 79: 2257-2270, 2019.
25. Curtis C, Shah SP, Chin SF, Turashvili G, Rueda OM, Dunning MJ, Speed D, Lynch AG, Samarajiwa S, Yuan Y, *et al*: The genomic and transcriptomic architecture of 2,000 breast tumours reveals novel subgroups. Nature 486: 346-352, 2012.
26. Zhao H, Langerod A, Ji Y, Nowels KW, Nesland JM, Tibshirani R, Bukholm IK, Karesen R, Botstein D, Borresen-Dale AL and Jeffrey SS: Different gene expression patterns in invasive lobular and ductal carcinomas of the breast. Mol Biol Cell 15: 2523-2536, 2004.
27. Jezequel P, Campone M, Gouraud W, Guerin-Charbonnel C, Leux C, Ricolleau G and Campion L: bc-GenExMiner: An easy-to-use online platform for gene prognostic analyses in breast cancer. Breast Cancer Res Treat 131: 765-775, 2012.
28. Jezequel P, Frenel JS, Campion L, Guerin-Charbonnel C, Gouraud W, Ricolleau G and Campone M: bc-GenExMiner 3.0: New mining module computes breast cancer gene expression correlation analyses. Database (Oxford) 2013: bas060, 2013.
29. Shen A, Liu L, Chen H, Qi F, Huang Y, Lin J, Sferra TJ, Sankararaman S, Wei L, Chu J, *et al*: Cell division cycle associated 5 promotes colorectal cancer progression by activating the ERK signaling pathway. Oncogenesis 8: 19, 2019.
30. Turowski TW, Lebaron S, Zhang E, Peil L, Dudnakova T, Petfalski E, Granneman S, Rappsilber J and Tollervey D: Rio1 mediates ATP-dependent final maturation of 40S ribosomal subunits. Nucleic Acids Res 42: 12189-12199, 2014.
31. He XW, Feng T, Yin QL, Jian YW and Liu T: NOB1 is essential for the survival of RKO colorectal cancer cells. World J Gastroenterol 21: 868-877, 2015.
32. Ruggero D: Revisiting the nucleolus: From marker to dynamic integrator of cancer signaling. Sci Signal 5: pe38, 2012.